



Published in final edited form as:

J Cell Physiol. 2017 December ; 232(12): 3775–3785. doi:10.1002/jcp.25857.

Irisin plays a pivotal role to protect the heart against ischemia and reperfusion injury:

A novel approach to inducing cardioprotection

Hao Wang^{1,*}, Yu Tina Zhao^{1,*}, Shouyan Zhang², Patrycja M Dubielecka³, Jianfeng Du¹, Naohiro Yano⁴, Y. Eugene Chin⁵, Shougang Zhuang³, Gangjian Qin⁶, and Ting C Zhao^{1,#}

¹Department of Surgery, Boston University Medical School, Roger Williams Medical Center, Providence, RI ²Department of Cardiology, Luoyang Central Hospital affiliated to Zhengzhou University, Luoyang, Henan, China ³Department of Medicine, Alpert Medical School, Brown University, Providence, Rhode Island ⁴Women and Infants Hospital, Brown University; Providence, RI ⁵Key Laboratory of Stem Cell Biology, Institutes of Health Sciences, Shanghai Institutes for Biological Sciences, Chinese Academy of Sciences, Shanghai, China ⁶Feinberg Cardiovascular Research Institute, Northwestern University Feinberg School of Medicine, Chicago

Abstract

Irisin, a newly identified hormone, is critical to modulating body metabolism, thermogenesis and reducing oxidative stresses. However, whether irisin protects the heart against myocardial ischemia and reperfusion (I/R) injury remains unknown. In this study, we determine the effect of irisin on myocardial I/R injury in the Langendorff perfused heart and cultured myocytes. Adult C57/BL6 mice were treated with irisin (100mg/kg) or vehicle for 30 minutes to elicit preconditioning. The isolated hearts were subjected to 30 min ischemia followed by 30 min reperfusion. Left ventricular function was measured and infarction size were determined using by tetrazolium staining. Western blot was employed to determine myocardial SOD-1, active-caspase 3, annexin V, p38 and phospho-p38. H9c2 cardiomyoblasts were exposed to hypoxia and reoxygenation for assessment of the effects of irisin on mitochondrial respiration and mitochondrial permeability transition pore (mPTP). Irisin treatment produced remarkable improvements in ventricular functional recovery, as evident by the increase in RPP and attenuation in LVEDP. As compared to the vehicle treatment, irisin resulted in a marked reduction of myocardial infarct size. Notably, irisin treatment increased SOD-1 and p38 phosphorylation, but suppressed levels of active-caspase 3, cleaved PARP, and annexin V. In cardiomyoblasts exposed to hypoxia/reoxygenation, irisin treatment significantly attenuated hypoxia/reoxygenation (H/R), as indicated by the reduction of lactate dehydrogenase (LDH) leakage and apoptotic cardiomyocytes. Furthermore, irisin treatments suppressed the opening of mPTP, mitochondrial swelling, and protected mitochondria function. Our results

#Corresponding Author: Ting C Zhao, MD, Associate Professor, Department of Surgery, Boston University Medical School, Roger William Medical Center, 50 Maude Street, Providence, RI 02908, tzhao@bu.edu, Fax: 401-456-2507, Tel: 401-456-8266.

*Equal contribution

Conflict of interests:

The authors declare that they have no competing interests.

indicate that irisin serves as a novel approach to eliciting cardioprotection, which is associated with the improvement of mitochondrial function.

Keywords

Irisin; Heart; Ischemia/Reperfusion; Cardioprotection

Introduction

Irisin is a recently identified proliferator-activated receptor-gamma coactivator-1 α (PGC γ -1 α)-dependent myokine, secreted by skeletal muscle and myocardium into circulation during exercise as a cleavage product of the extracellular portion of type I membrane protein fibronectin type III domain containing 5 (FNDC5) (Boström P et al., 2012). It was initially discovered as a kind of hormone responsible for the beneficial effects of exercise on the browning of white adipose tissues and increases in energy expenditure (Boström P et al., 2012). It has also been demonstrated to reduce oxidative stresses and apoptosis in different models (Zhu D et al., 2015; Park MJ et al., 2015). Recent evidence has indicated that irisin could induce the browning of white adipose tissue, which could be used as a therapeutic tool for metabolic disorders and cardiovascular diseases (Jeremic N et al., 2016). In an apoE(-/-) diabetic mice model, the systemic administration of irisin protected against endothelial injury and ameliorated atherosclerosis, indicating that irisin could be therapeutic for atherosclerotic vascular diseases in diabetes (Lu J et al., 2015). Additionally, decreased serum and vitreous irisin concentrations were found in type 2 diabetes mellitus patients (Hu W et al., 2016).

Irisin was demonstrated to be expressed abundantly in the muscle, heart (Li X et al., 2015). It was reported that irisin modulated the neurons in controlling the cardiac vagal tone through central cardiovascular regulation (Brailoiu E et al., 2015). Nevertheless, the significance and functional role of irisin in the modulation of myocardial ischemia and reperfusion injury are not clear. It is critical to define whether irisin could generate a protective effect against myocardial ischemia and reperfusion injury, which could be developed as a novel strategy in the treatment of cardiovascular disease and other pathological disorders. Furthermore, whether specific signaling pathway and mitochondrial function are involved in irisin-induced cardioprotective effects remain unknown. Therefore, in this study, we employed an isovolumetrically perfused heart, a well-established myocardial ischemia and reperfusion model, and *in vitro* hypoxia/reoxygenation cell culture model to determine 1) whether irisin treatment could increase the resistance of the heart against I/R injury by improving post-ischemic functional recovery and reducing infarct size in ex vivo perfused heart; 2) whether irisin-induced protective effects are associated with a unique signaling pathway; 3) whether the irisin-induced protective effect is closely associated with the preservation of mitochondrial function in cardiomyoblasts exposed to hypoxia/reoxygenation. These results suggest that irisin generated a protective effect against myocardial ischemic injury as demonstrated by the improvement of post-ischemic ventricular function and reduction of infarct size, which were associated with the

suppression of the opening of mPTP, mitochondrial swelling, and protected mitochondria function.

Materials and Methods

Animals and cell culture

Two-month old C57/BL6 mice were obtained from Jackson Laboratory (Bar Harbor, Maine). All animal experiments were conducted under a protocol approved by the Institutional Animal Care and Use Committee of Institute, which conforms to the Guide for the Care and Use of Laboratory Animals published by the US National Institutes of Health (NIH Publication No. 85-23, revised 1996). H9C2 cardiomyoblasts were purchased from American Type Culture Collection (ATCC, Manassas, VA). Cells were cultured in Dulbecco's Modified Eagle Medium (DMEM) supplemented with 10% heat-inactivated fetal bovine serum (FBS) and 1% penicillin/streptomycin at 37°C in a humidified atmosphere of 5% CO₂.

Reagents and antibodies

Irisin was purchased from Cayman Chemical (Michigan, USA). All chemicals for the heart perfusion and mitochondria isolation were purchased from Sigma-Aldrich (St. Louis, MO). The MitoCapture mitochondrial apoptosis detection kit was obtained from BioVision (Tokyo, Japan). Active-caspase 3 and cleaved PARP polyclonal rabbit antibodies were obtained from Abcam (MA, USA). Irisin primary antibody was purchased from Cayman Chemical (Michigan, USA). Primary antibodies including polyclonal rabbit β -actin, polyclonal rabbit p38, polyclonal rabbit phosphor-p38, Erk, phosphorylated Erk and polyclonal rabbit superoxide dismutase (SOD-1) were purchased from Santa Cruz Biotechnology (Santa Cruz, CA).

Langendorff isolated heart perfusion

The methodologies of Langendorff perfused system and ventricular function detection have been described previously (Zhao TC et al., 2013). Briefly, mice were anesthetized with an intraperitoneal injection (i.p.) of pentobarbital sodium (120 mg/kg). The hearts were excised and arrested in ice-cold Krebs-Henseleit buffer (K-H), then cannulated via the ascending aorta for retrograde perfusion in the Langendorff system, which was aerated with 95% O₂:5% CO₂ to maintain a pH value of 7.4 at 37°C, with a constant perfusion pressure of 55 mmHg. A water-filled latex balloon, attached to the tip of polyethylene tubing, was then inflated sufficiently to provide a left ventricular end-diastolic pressure (LVEDP) of about 10 mmHg. Myocardial function was measured including left ventricular systolic pressure (LVSP), dp/dt max, dp/dt min, heart rate (HR), and coronary flow (CF). Left ventricular developed pressure (LVDP) was calculated by subtracting LVEDP from peak systolic pressure. Rate pressure product (RPP), an index of cardiac work, was calculated by multiplying LVDP with HR.

Measurement of Myocardial Infarction

The infarction size was measured with a modification as previously described with 10% triphenyltetrazolium chloride staining (Zhao TC and Kukreja RC 2003). The infarct size was

calculated and presented as the percentage of risk area, defined as the sum of total ventricular area minus cavities.

Experimental protocol for myocardial I/R injury

Mice were randomized into three experimental groups as shown in Figure 1. Mice were randomly divided into 3 groups as follows (8–9 per group): 1) **Control group**: mice did not receive treatment with either vehicle or irisin, the hearts were isolated and perfused for 70 min in K-H buffer; 2) **I/R group** mice received an intraperitoneal (i.p.) injection of 0.1 ml vehicle (saline). 30 minutes later, hearts were subjected to 10 minutes of equilibration and 30 minutes ischemia followed by 30 minutes reperfusion; 3) **Irisin +I/R group**: Mice received an i.p. injection of irisin (100mg/kg) to elicit pharmacological preconditioning, then hearts were subjected to I/R as above.

Another subset of animals including I/R were treated with or without irisin solely for the purpose of measuring active-caspase-3, SOD-1, phosphorylated-p38, and Erk signaling pathways. Animals were treated with irisin as described above, and cardiac tissues were collected after 30 min following treatments.

Hypoxia/reoxygenation (H/R) protocol in vitro H9c2 cardiomyoblasts

The protocol of cardiomyoblasts exposed to hypoxia/reoxygenation was described as before (Ju J et al., 2015). Briefly, cultured H9c2 cardiomyoblasts were pretreated with or without irisin (10ng/ml) for 2 h, cells were subjected to either normoxia or hypoxia in a hypoxic chamber (1% O₂, 5% CO₂ and 94% N₂) for 2 h followed by 1 h of reoxygenation. Cell viability, death, apoptosis and mitochondrial functions were examined using the methods described afterwards.

Lactate dehydrogenase (LDH) leakage detection

Supernatants from H9c2 cardiomyoblast culture medium were collected to detect LDH leakage, which was described in the previous section (Zhao TC et al., 2010). The release of LDH was determined using a commercially available kit (Roche), as per the manufacturer's protocol with a modification (Tantini B et al., 2006).

Immunochemical staining

Immunostaining was performed as described in detail in our previous studies (Tseng A et al., 2010; Zhang L et al 2012). H9c2 cardiomyoblasts were fixed via 4% paraformaldehyde and then blocked with the incubation of polyclonal anti-active caspase 3 antibody (Abcam, Cambridge, MA), which was followed by goat anti-rabbit Alexa Fluor 555 secondary antibody (Life Technologies). The percentage of apoptotic positive cells was determined in five randomly chosen fields and was normalized with the total number of stained nuclei by DAPI.

Western blot

The methods and details for protein preparations and immunoblotting were carried out as before (Zhang L et al., 2012). In brief, the blots were incubated with their respective

polyclonal antibodies, including p38 polyclonal, phospho-p38 polyclonal, Erk polyclonal, phospho-Erk polyclonal, SOD-1 polyclonal, active-caspase 3 polyclonal, irisin polyclonal and β -actin monoclonal antibodies at a dilution concentration of 1:1,000, then visualized by anti-rabbit or anti-mouse horseradish peroxidase-conjugated secondary antibody (1:2,000), and finally developed with ECL chemiluminescence detection reagent (Amersham Pharmacia Biotech).

Real time polymerase chain reaction (PCR)

Total myocardial RNA was extracted from different groups with Trizol reagent (Life Technologies, Grand Island, NY). cDNA was synthesized from 5 μ g of total RNA. The reverse transcribed cDNA (5 μ L) was amplified to a final volume of 50 μ L by PCR under standard conditions. Real-time PCR experiments were performed on a master cycler realplex4 (Eppendorf North America) system using qPCR Kit master mix (Kapabiosystems, Boston, USA). Irisin: Forward: GAACAAAGATGAGGTGACCA; Reverse: ACCACAACAATGATCAGCA. GAPDH was used as the internal control. Three hearts in each group were utilized to determine mRNA content.

Mitochondrial membrane potential

A reduction in mitochondrial membrane potential is an early indicator of apoptosis induction (Yoon JC et al., 2014). MitoCapture apoptosis was detected using MitoCapture mitochondrial apoptosis kit according to protocols provided by the manufacturer (DeNicola M et al., 2014; Takai N et al., 2008). Briefly, after the cardiomyoblasts were treated with H/R described above, the cells were incubated in 1 ml of incubation buffer containing 1 μ L of MitoCapture for 20 min at 37°C in an incubator. The fluorescent signals were measured with a microscope. The red fluorescent signals were excited at 530 nm and detected at 630 nm, and the green fluorescence was excited at 488 nm and detected at 530 nm.

Mitochondrial permeability transition pore (mPTP)

mPTP opening was measured by using the method described previously (DeNicola M et al., 2014; Bernardi P et al., 1999). In brief, the cells were washed with Hanks' balanced salt solution-10 mM HEPES (pH 7.2) before staining with 1 μ mol/l calcein-AM (Molecular Probes) in the presence of 8 mmol/l cobalt chloride (CoCl_2) at room temperature for 20 min in darkness. CoCl_2 was added to quench the cytoplasmic signal so that only the fluorescence mitochondria were captured. Change in fluorescence intensity is an index of mPTP opening, and integrated optical density was obtained from three to four independent experiments.

Measurement of mitochondrial swelling

Mitochondrial isolation was carried out with the modification as described as previously (Kristal BS et al, 1996). At the end of experiments, cells were collected, washed with PBS buffer, and placed in ice-cold buffer (250 mM mannitol, 75 mM sucrose, 100 μ M EDTA, and 10 mM HEPES, pH 7.4) supplemented with 500 μ M EGTA. Following homogenization, cell extracts were centrifuged at 1000 $\times g$ for 10 min. Then, cell supernatants were removed and centrifuged at 10,000 $\times g$ for 15 min. Pellets were washed twice in buffer as above supplemented with 0.5% fatty acid free bovine serum albumin and re-spun at 10,000 rpm.

Following the final wash, mitochondria were re-suspended in buffer ice cold buffer as described above. Mitochondrial swelling was induced by 50 μ M of clacium, where the light-scattering of 65 μ g of mitochondria in a 1-mL volume was measured at 540 nm for 6 min (Lam CK et al., 2015).

Statistical analysis

All data are expressed as mean \pm SEM. Differences among groups were analyzed by one-way analysis of variance (ANOVA), followed by Bonferroni correction. A $p<0.05$ was considered to be of statistical significance.

Results

Ventricular function in the baseline

As shown in Table 1, the baseline cardiac function parameters, including LVSP, LVDP, LVEDP, rate pressure product (RPP), dp/dt max, dp/dt min, heart rate (HR) and coronary flow (CF), exhibited no significant differences between control, I/R and Irisin+I/R group before I/R.

Irisin Improves Post-Ischemic Ventricular Functional Recovery

As shown in Figures 2A and B, following reperfusion, post-ischemic myocardial function exhibits a gradual recovery in different treatments. However, during the course of reperfusion, irisin treatment demonstrates a better recovery of LVDP, LVEDP, RPP, dp/dt max, and dp/dt min as compared to I/R group. At the end of reperfusion, as shown in Figures 2A and 2B and Supplemental Figures 1A and B, LVDP was 65.3 \pm 3.5 mmHg in the I/R group, which was significantly improved as compared with the irisin treatment group (91 \pm 7.6 mmHg, $p<0.001$). In addition, irisin treatment also induced an improvement in LVSP (from 83 \pm 4.7mmHg to 100.4 \pm 5.0 mmHg, $p<0.05$) and RPP (from 22.6 \pm 1.7 $\times 10^3$ mmHg/s to 29.8 \pm 2.7 $\times 10^3$ mm Hg/s, $p<0.05$). The post-ischemic LVEDP (in mmHg) was decreased from 17.7 \pm 2.2 in the vehicle group to 9.3 \pm 2.4 in irisin treatment group ($p<0.001$). Likewise, a significant improvement was observed in dp/dt max recovery (from 1930 \pm 94.0 mmHg/s $\times 10^{-3}$ in I/R to 2465 \pm 203.4 mmHg/s $\times 10^{-3}$ in irisin treatment, $p<0.001$). There were no significant differences in heart rate between the groups and but there was a better coronary flow recovery following irisin treatment (Figure 2B). Representative images of myocardial functions were shown in Figure 2C. Taken together, the post-ischemic recovery of ventricular function was significantly improved by irisin treatment (Figure 2, Supplemental Figures 1C & D).

Irisin reduces infarction size of hearts after I/R

Myocardial infarct size, an index of irreversible myocardial injury, was assessed. As shown in Figure 3A, irisin-treated mice demonstrated a significantly larger area of viable tissue in the post-ischemic heart (brick red color) compared with the vehicle-treated controls, which had much larger gray and white areas. As shown in Figure 3B, the infarct size was reduced from 48.85 \pm 2.28% in the I/R group to 36.04 \pm 3.13% ($p<0.05$) in the irisin group. There was no difference in risk area between the groups.

Irisin treatment reduces myocardial apoptosis and oxidative stress

As shown in Figures 4 A and B, a significant decrease in active-caspase 3 was observed in the irisin group as compared with the I/R group. Furthermore, as shown in Figures 4 A and C, cleaved PARP was elevated following I/R, but irisin treatment attenuated the cleaved PARP content. In addition, as shown in Figure 4D, the western blot showed decreased Annexin V and an increased SOD-1 levels following irisin treatment compared to I/R control mice. Likewise, as shown in Supplemental Figures 2A and B, I/R increased annexin V positive nuclei as compared to the control, whereas irisin treatment significantly reduced annexin V positive-nuclei in myocardial sections. These results indicate that irisin treatment suppressed myocardial apoptosis and oxidative stress. We have previously shown that preconditioning could elicit p38 phosphorylation (Zhao TC et al., 2007). As shown in Figure 4 E, phosphorylated p38 was expressed at relatively low levels in the vehicle-treated mice. However, irisin treatment significantly promoted the expression of phosphorylated-p38. In contrast, as shown in Figure 4F, irisin resulted in the reduction of phosphorylated Erk1/2. In addition, as shown in Figure 4G and H, irisin mRNA and protein levels in the myocardium significantly increased after I/R stress, suggesting that irisin increased in response to I/R injury.

Irisin reduced cell cytotoxicity in H9c2 cardiomyoblasts exposed to hypoxia/reoxygenation

The effects of irisin in hypoxia/reoxygenation was examined by measuring the release of the cytosolic LDH enzyme to indicate cell death by necrosis (Bernuzzi F et al., 2009; Sardão VA et al., 2009). The measurement was carried out in cells subjected to 2h hypoxia and followed by 1h normoxia (Figure 5A). As shown in Figure 5B, LDH release increased from 21.8% to 37.4% after oxidative stress ($p < 0.01$). LDH leakage was significantly reduced to 29.2% in the irisin-treated hypoxia/reoxygenation group ($p < 0.05$ vs. control H/R).

As shown in Figure 6 A and B, active-caspase 3 was highly exhibited in cardiomyoblasts exposed to hypoxia/reoxygenation injury, which increased from $4.8\% \pm 1.4\%$ in normoxia to $79.8\% \pm 5.1\%$ with hypoxia/reoxygenation ($p < 0.001$). Notably, the percent of apoptotic cells was reduced to $26.3\% \pm 4.0\%$ by irisin treatment as compared to control hypoxia/reoxygenation ($p < 0.001$), suggesting that irisin protected the cells against apoptosis induced by hypoxia/reoxygenation, which supports the results observed in I/R hearts.

Irisin protects H9c2 cells from hypoxia/reoxygenation induced mitochondrial damage

Modification of the mitochondrial membrane potential (MTP) is an early event in the induction of apoptosis. As shown in Figure 7A, H9c2 cardiomyoblasts lost the red fluorescent signals in cells exposed to hypoxia/reoxygenation. However, hypoxia/reoxygenation-elicited MTP loss was significantly prevented by irisin treatment, indicating that irisin-induced cellular protection is highly related to the maintenance of MTP.

Irisin inhibited the mPTP opening

The mitochondrial permeability transition pore (mPTP) plays a critical role in the pathogenesis of myocardial ischemia/reperfusion injury (Weiss JN et al 2003; Suleiman MS

et al., 2001). Inhibition of the mPTP opening at early reperfusion was shown to protect the heart from reperfusion (Halestrap AP et al., 2004; Argaud L et al 2005). As shown in Figure 7B–C, mitochondrial green fluorescence signals were significantly lost in cells exposed to hypoxia/reoxygenation injury, which was improved by irisin treatment. Furthermore, as shown in Figure 7D, the effects of irisin on mitochondrial integrity were also evidenced upon calcium loading, a situation that induced the opening of the mitochondrial permeability transition pore, resulting in failures of osmotic pressure control, water fluxes and mitochondrial swelling. Upon calcium loading, hypoxia and reoxygenation caused a loss of light scattered by the mitochondrial member structure. However, irisin treatment demonstrated resistance under an identical condition and significantly reduced the magnitude of mitochondrial swelling.

Discussion

Salient findings and perspectives

To the best of our knowledge, this study is the first demonstration that irisin protected the heart against ischemia and reperfusion injury by improving post-ischemic ventricular functional recovery as well as a reduction of infarct size. The protective effects of irisin were also associated with the attenuation of active caspase-3, cleaved PARP, which then increased SOD-1 and p38 phosphorylation. Furthermore, irisin increased the resistance of cardiomyoblasts exposed to hypoxia/reoxygenation, which was closely related to suppression of mitochondrial apoptosis, inhibition of mitochondrial PTP, and suppression of mitochondrial swelling. Taken together, irisin plays a critical role in protecting the heart against ischemia and reperfusion injury, attenuating of apoptosis, and improving mitochondrial function.

Irisin is a recently identified hormone, which is produced by the proteolytic processing of a transmembrane receptor, fibronectin domain-containing protein 5 (FNDC5) (Huh JY et al., 2012; Polyzos SA et al., 2013), highly expressed in skeletal muscle, pericardium, heart, and brain (Wrann CD et al., 2013). It contains a 209-residue protein with an N-terminal 29-residue signal sequence, followed by the irisin or putative fibronectin III (FNIII) 2 domain, a linking peptide, a transmembrane domain, and a 39-residue cytoplasmic segment (Raschke S et al., 2013; Ferrer-Martínez A et al., 2002), which functions as a myokine by binding to an unknown receptor (Schumacher MA et al., 2013).

Evidence has indicated the significant effects of irisin on the body metabolism and thermogenesis (Boström P et al., 2012; Spiegelman BM and Banting Lecture, 2013; Rachid TL et al 2015). The beneficial effects of irisin on metabolism syndromes include not only the driving of the browning of white adipose tissue and then increasing the energy expenditure, but also include suppressing inflammation and oxidative stress induced by, for example, high circulation of glucose and obesity (Zhu D et al., 2015; Dulian K et al., 2015; Polyzos SA et al., 2015; Lu J et al., 2015). Although irisin was recently identified as an important molecule in attenuating metabolic disorders, its functional role in modulating cardiac ischemia and reperfusion has not been defined recently. Identification of irisin in regulation of myocardial I/R injury using this model will also provide new insight to understanding its protective function of irisin in other organs. An increased level of irisin in

response to I/R indicates the potential importance of irisin for modulation of I/R. Pretreatment of irisin attenuated myocardial infarct size and improved post-ischemic functional recovery, indicating that irisin produces a cardioprotective effect. It was reported that the pacing protocol was utilized in the isovolumetric heart to determine cardiac function (Taylor PB and Cerny FJ, 1976). In this observation, we used a well-established approach to evaluate myocardial function as described previously, which is considered to exclude the potential role of preconditioning effect by pacing (Zhao TC et al, 2001). Irisin induced the reductions of active caspase-3, cleaved PARP, and annexin V in this study, which indicates that anti-apoptosis plays an essential role for irisin-induced protection. Additionally, it is known that protective effects against myocardial I/R injury are associated with increased anti-oxidant function (Tamura Y et al., 1988). An increase in SOD-1 following irisin-treatment suggests that the increased anti-oxidant role is responsible for the function of irisin-elicited protection.

We and others previously reported that the reduced rate of mitochondrial respiration capacity contributes to impairment of mitochondrial function and cardiac function (DeNicola M, et al., 2014; Boudina S et al., 2005). Earlier observations demonstrated that hypoxia triggers mitochondrial perturbations and cell deaths of cardiomyocytes (Baetz D et al., 2005). The present study shows that cardiomyoblasts exhibited increased mPTP, mitochondrial swelling, and mitochondrial apoptosis in response to hypoxia/reoxygenation, which was reduced by Irisin treatment. In line with this observation, our previous report also indicates the protective effects of inhibiting mPTP and suppressing mitochondrial apoptosis in the stimulation of glucagon-like peptide-1 receptor-induced protective effects in cardiomyocytes (DeNicola M, et al., 2014). This suggests that modulation of mitochondrial function is critical for irisin-generated cellular protective effects. Although our studies demonstrated that irisin attenuated cell death under hypoxia, we did not estimate the effect of irisin on cell necrosis, which is a limitation and holds merit for future investigations.

MAPK plays an important role in the transmission of signals from cell surface receptors and the environment (Bozkurt B et al., 1998; Rose BA 2010). Activation of p38 is associated with cardiac protection (Baines CP et al., 1999; Mackay K and Mochly-Rosen D, 1999; Carini R et al., 2001; Han J et al., 1994; Zhao TC et al., 2001). p38 activation triggered delayed cardioprotection in ischemic hearts under pharmacologic preconditioning (Zhao TC et al., 2001; Zhao TC et al., 2001). In this study, we have found that irisin treatment increased p38 phosphorylation in the myocardium, which is in agreement with an observation in which irisin upregulated uncoupling protein-1 through phosphorylation of the p38 (Zhang Y et al., 2014). Likewise, it was also demonstrated that irisin modulated glucose uptake in skeletal muscle through the MAPK/p38 pathway (Lee HJ et al, 2015). However, Erk phosphorylation was attenuated in the irisin treated group, indicating that the cardiac protective effects of irisin against I/R injured hearts is related to the activation of p38, but not Erk phosphorylation. It is not clear whether the effect of irisin on Erk phosphorylation is also related to the difference in animal models. It is also interesting to utilize the genetic approach to define the cause and effect relationship of these kinase with irisin-induced protection in the future.

In conclusion, this study has demonstrated that irisin protects the heart against ischemia and reperfusion injury, as indicated by an improvement in post-ischemic ventricular function, increase in recovery of coronary effluent, and reduction of infarct size. Ischemia stimulates the increase in transcriptional and protein levels of irisin in the myocardium. Furthermore, irisin decreased apoptotic proteins including active caspase 3, cleaved PARP, and annexin V and elicited increases in p38 phosphorylation and SOD-1 in the post-ischemic myocardium. Furthermore, irisin increased the resistance of cardiomyoblasts exposed to hypoxia and reoxygenation, which is closely associated with the attenuation of mPTP opening, mitochondrial swelling, and mitochondrial apoptosis. Taken together, our results demonstrate that irisin acts as a novel approach to inducing protection against ischemic injury, which holds promise in developing a new therapeutic strategy in cardiac protection.

Supplementary Material

Refer to Web version on PubMed Central for supplementary material.

Acknowledgments

The work is supported by the National Heart, Lung, and Blood Institute Grant (R01 HL089405 and R01 HL115265).

References

1. Argaud L, Gateau-Roesch O, Raissy O, Loufouat J, Robert D, Ovize M. Postconditioning inhibits mitochondrial permeability transition. *Circulation*. 2005; 111(2):194–7. [PubMed: 15642769]
2. Baines CP, Liu GS, Birincioglu M, Critz SD, Cohen MV, Downey JM. Ischemic preconditioning depends on interaction between mitochondrial KATP channels and actin cytoskeleton. *Am J Physiol*. 1999; 276(4 Pt 2):H1361–8. [PubMed: 10199863]
3. Baetz D, Regula KM, Ens K, Shaw J, Kothari S, Yurkova N, Kirshenbaum LA. Nuclear factor-kappaB-mediated cell survival involves transcriptional silencing of the mitochondrial death gene BNIP3 in ventricular myocytes. *Circulation*. 2005; 112(24):3777–85. [PubMed: 16344406]
4. Bernardi P, Scorrano L, Colonna R, Petronilli V, Di Lisa F. Mitochondria and cell death. Mechanistic aspects and methodological issues. *Eur J Biochem*. 1999; 264(3):687–701. [PubMed: 10491114]
5. Bernuzzi F, Recalcati S, Alberghini A, Cairo G. Reactive oxygen species-independent apoptosis in doxorubicin-treated H9c2 cardiomyocytes: role for heme oxygenase-1 down-modulation. *Chem Biol Interact*. 2009; 177(1):12–20. [PubMed: 18845130]
6. Boström P, Wu J, Jedrychowski MP, Korde A, Ye L, Lo JC, Rasbach KA, Boström EA, Choi JH, Long JZ, Kajimura S, Zingaretti MC, Vind BF, Tu H, Cinti S, Højlund K, Gygi SP, Spiegelman BM. A PGC1- α -dependent myokine that drives brown-fat-like development of white fat and thermogenesis. *Nature*. 2012; 481(7382):463–8. [PubMed: 22237023]
7. Boudina S, Sena S, O'Neill BT, Tathireddy P, Young ME, Abel ED. Reduced mitochondrial oxidative capacity and increased mitochondrial uncoupling impair myocardial energetics in obesity. *Circulation*. 2005; 112(17):2686–95. [PubMed: 16246967]
8. Bozkurt B, Kribbs SB, Clubb FJ Jr, Michael LH, Didenko VV, Hornsby PJ, Seta Y, Oral H, Spinale FG, Mann DL. Pathophysiologically relevant concentrations of tumor necrosis factor- α promote progressive left ventricular dysfunction and remodeling in rats. *Circulation*. 1998; 97(14):1382–91. [PubMed: 9577950]
9. Brailoiu E, Deliu E, Sporici RA, Brailoiu GC. Irisin evokes bradycardia by activating cardiac-projecting neurons of nucleus ambiguus. *Physiol Rep*. 2015; 3(6) pii: e12419.

10. Carini R, De Cesaris MG, Splendore R, Vay D, Domenicotti C, Nitti MP, Paola D, Pronzato MA, Albano E. Signal pathway involved in the development of hypoxic preconditioning in rat hepatocytes. *Hepatology*. 2001; 33(1):131–9. [PubMed: 11124829]
11. DeNicola M, Du J, Wang Z, Yano N, Zhang L, Wang Y, Qin G, Zhuang S, Zhao TC. Stimulation of glucagon-like peptide-1 receptor through exendin-4 preserves myocardial performance and prevents cardiac remodeling in infarcted myocardium. *Am J Physiol Endocrinol Metab*. 2014; 307(8):E630–43. [PubMed: 25117407]
12. Dulian K, Laskowski R, Grzywacz T, Kujach S, Flis DJ, Smaruj M, Ziemann E. The whole body cryostimulation modifies irisin concentration and reduces inflammation in middle aged, obese men. *Cryobiology*. 2015; 71(3):398–404. [PubMed: 26475491]
13. Du J, Zhang L, Zhuang S, Qin GJ, Zhao TC. HDAC4 degradation mediates HDAC inhibition-induced protective effects against hypoxia/reoxygenation injury. *J Cell Physiol*. 2015; 230(6): 1321–31. [PubMed: 25475100]
14. Ferrer-Martínez A, Ruiz-Lozano P, Chien KR, Mouse PeP. a novel peroxisomal protein linked to myoblast differentiation and development. *Dev Dyn*. 2002; 224(2):154–67. [PubMed: 12112469]
15. Halestrap AP, Clarke SJ, Javadov SA. Mitochondrial permeability transition pore opening during myocardial reperfusion—a target for cardioprotection. *Cardiovasc Res*. 2004; 61(3):372–85. [PubMed: 14962470]
16. Han J, Lee JD, Bibbs L, Ulevitch RJ. A MAP kinase targeted by endotoxin and hyperosmolarity in mammalian cells. *Science*. 1994; 265(5173):808–11. [PubMed: 7914033]
17. Huh JY, Panagiotou G, Mougios V, Brinkoetter M, Vamvini MT, Schneider BE, Mantzoros CS. FNDC5 and irisin in humans: I. Predictors of circulating concentrations in serum and plasma and II. mRNA expression and circulating concentrations in response to weight loss and exercise. *Metabolism*. 2012; 61(12):1725–38. [PubMed: 23018146]
18. Hu W, Wang R, Li J, Zhang J, Wang W. Association of irisin concentrations with the presence of diabetic nephropathy and retinopathy. *Ann Clin Biochem*. 2016; 53(Pt 1):67–74. [PubMed: 25814621]
19. Jeremic N, Chatuverdi P, Tyagi SC. Browning of White Fat: Novel Insight into Factors, Mechanisms and Therapeutics. *J Cell Physiol*. 2017; 232(1):61–8. [PubMed: 27279601]
20. Kristal BS, Park BK, Yu BP. 4-Hydroxyhexenal is a potent inducer of the mitochondrial permeability transition. *J Biol Chem*. 1996; 271(11):6033–8. [PubMed: 8626387]
21. Lam CK, Zhao W, Liu GS, Cai WF, Gardner G, Adly G, Kranias EG. HAX-1 regulates cyclophilin-D levels and mitochondria permeability transition pore in the heart. *Proc Natl Acad Sci U S A*. 2015; 112(47):E6466–75. [PubMed: 26553996]
22. Li X, Fang W, Hu Y, Wang Y, Li J. Characterization of fibronectin type III domain-containing protein 5 (FNDC5) gene in chickens: Cloning, tissue expression, and regulation of its expression in the muscle by fasting and cold exposure. *Gene*. 2015; 570(2):221–9. [PubMed: 26072164]
23. Lu J, Xiang G, Liu M, Mei W, Xiang L, Dong J. Irisin protects against endothelial injury and ameliorates atherosclerosis in apolipoprotein E-Null diabetic mice. *Atherosclerosis*. 2015; 243(2): 438–48. [PubMed: 26520898]
24. Mackay K, Mochly-Rosen D. An inhibitor of p38 mitogen-activated protein kinase protects neonatal cardiac myocytes from ischemia. *J Biol Chem*. 1999; 274(10):6272–9. [PubMed: 10037715]
25. Park MJ, Kim DI, Choi JH, Heo YR, Park SH. New role of irisin in hepatocytes: The protective effect of hepatic steatosis in vitro. *Cell Signal*. 2015; 27(9):1831–9. [PubMed: 25917316]
26. Polyzos SA, Kountouras J, Anastasilakis AD, Geladari EV, Mantzoros CS. Irisin in patients with nonalcoholic fatty liver disease. *Metabolism*. 2014; 63(2):207–17. [PubMed: 24140091]
27. Polyzos SA, Kountouras J, Shields K, Mantzoros CS. Irisin: a renaissance in metabolism? *Metabolism*. 2013; 62(8):1037–44. [PubMed: 23664085]
28. Rachid TL, Penna-de-Carvalho A, Bringhenti I, Aguila MB, Mandarim-de-Lacerda CA, Souza-Mello V. Fenofibrate (PPARalpha agonist) induces beige cell formation in subcutaneous white adipose tissue from diet-induced male obese mice. *Mol Cell Endocrinol*. 2015; 402:86–94. [PubMed: 25576856]

29. Raschke S, Elsen M, Gassenhuber H, Sommerfeld M, Schwahn U, Brockmann B, Jung R, Wisløff U, Tjønnå AE, Raastad T, Hallén J, Norheim F, Drevon CA, Romacho T, Eckardt K, Eckel J. Evidence against a beneficial effect of irisin in humans. *PLoS One*. 2013; 8(9):e73680. [PubMed: 24040023]
30. Rose BA, Force T, Wang Y. Mitogen-activated protein kinase signaling in the heart: angels versus demons in a heart-breaking tale. *Physiol Rev*. 2010; 90(4):1507–46. [PubMed: 20959622]
31. Sardão VA, Oliveira PJ, Holy J, Oliveira CR, Wallace KB. Morphological alterations induced by doxorubicin on H9c2 myoblasts: nuclear, mitochondrial, and cytoskeletal targets. *Cell Biol Toxicol*. 2009; 25(3):227–43. [PubMed: 18386138]
32. Schumacher MA, Chinnam N, Ohashi T, Shah RS, Erickson HP. The structure of irisin reveals a novel intersubunit β -sheet fibronectin type III (FNIII) dimer: implications for receptor activation. *J Biol Chem*. 2013; 288(47):33738–44. [PubMed: 24114836]
33. Spiegelman BM. Banting Lecture 2012: 2013. Regulation of adipogenesis: toward new therapeutics for metabolic disease. *Diabetes*. 62(6):1774–82.
34. Taylor PB, Cerny FJ. Evaluation of the isolated paced rat heart. *J Appl Physiol*. 1976; 41:328–331. [PubMed: 965300]
35. Tamura Y, Chi LG, Driscoll EM Jr, Hoff PT, Freeman BA, Gallagher KP, Lucchesi BR. Superoxide dismutase conjugated to polyethylene glycol provides sustained protection against myocardial ischemia/reperfusion injury in canine heart. *Circ Res*. 1988; 63(5):944–59. [PubMed: 3180357]
36. Tantini B, Fiumana E, Cetrullo S, Pignatti C, Bonavita F, Shantz LM, Giordano E, Muscari C, Flamigni F, Guarnieri C, Stefanelli C, Caldarera CM. Involvement of polyamines in apoptosis of cardiac myoblasts in a model of simulated ischemia. *J Mol Cell Cardiol*. 2006; 40(6):775–82. [PubMed: 16678846]
37. Takai N, Ueda T, Nishida M, Nasu K, Narahara H. Bufalin induces growth inhibition, cell cycle arrest and apoptosis in human endometrial and ovarian cancer cells. *Int J Mol Med*. 2008; 21(5): 637–43. [PubMed: 18425357]
38. Tseng A, Stabila J, McGonnigal B, Yano N, Yang MJ, Tseng YT, Davol PA, Lum LG, Padbury JF, Zhao TC. Effect of disruption of Akt-1 of lin(-)c-kit(+) stem cells on myocardial performance in infarcted heart. *Cardiovasc Res*. 2010; 87(4):704–12. [PubMed: 20410290]
39. Suleiman MS, Halestrap AP, Griffiths EJ. Mitochondria: a target for myocardial protection. *Pharmacol Ther*. 2001; 89(1):29–46. [PubMed: 11316512]
40. Weiss JN, Korge P, Honda HM, Ping P. Role of the mitochondrial permeability transition in myocardial disease. *Circ Res*. 2003; 93(4):292–301. [PubMed: 12933700]
41. Wrann CD, White JP, Salogiannis J, Laznik-Bogoslavski D, Wu J, Ma D, Lin JD, Greenberg ME, Spiegelman BM. Exercise induces hippocampal BDNF through a PGC-1 α /FNDC5 pathway. *Cell Metab*. 2013; 18(5):649–59. [PubMed: 24120943]
42. Yoon JC, Ling AJ, Isik M, Lee DY, Steinbaugh MJ, Sack LM, Boduch AN, Blackwell TK, Sinclair DA, Elledge SJ. GLTSCR2/PICT1 links mitochondrial stress and Myc signaling. *Proc Natl Acad Sci U S A*. 2014; 111(10):3781–6. [PubMed: 24556985]
43. Zhang L, Qin X, Zhao Y, Fast L, Zhuang S, Liu P, Cheng G, Zhao TC. Inhibition of histone deacetylases preserves myocardial performance and prevents cardiac remodeling through stimulation of endogenous angiomyogenesis. *J Pharmacol Exp Ther*. 2012; 341(1):285–93. [PubMed: 22271820]
44. Zhang Y, Li R, Meng Y, Li S, Donelan W, Zhao Y, Qi L, Zhang M, Wang X, Cui T, Yang LJ, Tang D. Irisin stimulates browning of white adipocytes through mitogen-activated protein kinase p38 MAP kinase and ERK MAP kinase signaling. *Diabetes*. 2014; 63(2):514–25. [PubMed: 24150604]
45. Zhao TC, Cheng G, Zhang LX, Tseng YT, Padbury JF. Inhibition of histone deacetylases triggers pharmacologic preconditioning effects against myocardial ischemic injury. *Cardiovasc Res*. 2007; 76(3):473–81. [PubMed: 17884027]
46. Zhao TC, Du J, Zhuang S, Liu P, Zhang LX. HDAC inhibition elicits myocardial protective effect through modulation of MKK3/Akt-1. *PLoS One*. 2013; 8(6):e65474. [PubMed: 23762381]
47. Zhao TC, Hines DS, Kukreja RC. Adenosine-induced late preconditioning in mouse hearts: role of p38 MAP kinase and mitochondrial K(ATP) channels. *Am J Physiol Heart Circ Physiol*. 2001; 280(3):H1278–85. [PubMed: 11179074]

48. Zhao TC, Kukreja RC. Protein kinase C-delta mediates adenosine A3 receptor-induced delayed cardioprotection in mouse. *Am J Physiol Heart Circ Physiol.* 2003; 285(1):H434–41. [PubMed: 12793983]
49. Zhao TC, Taher MM, Valerie KC, Kukreja RC. p38 Triggers late preconditioning elicited by anisomycin in heart: involvement of NF-kappaB and iNOS. *Circ Res.* 2001; 89(10):915–22. [PubMed: 11701619]
50. Zhao TC, Zhang LX, Cheng G, Liu JT. gp-91 mediates histone deacetylase inhibition-induced cardioprotection. *Biochim Biophys Acta.* 2010; 1803(7):872–80. [PubMed: 20433879]
51. Zhu D, Wang H, Zhang J, Zhang X, Xin C, Zhang F, Lee Y, Zhang L, Lian K, Yan W, Ma X, Liu Y, Tao L. Irisin improves endothelial function in type 2 diabetes through reducing oxidative/nitrative stresses. *J Mol Cell Cardiol.* 2015; 87:138–47. [PubMed: 26225842]

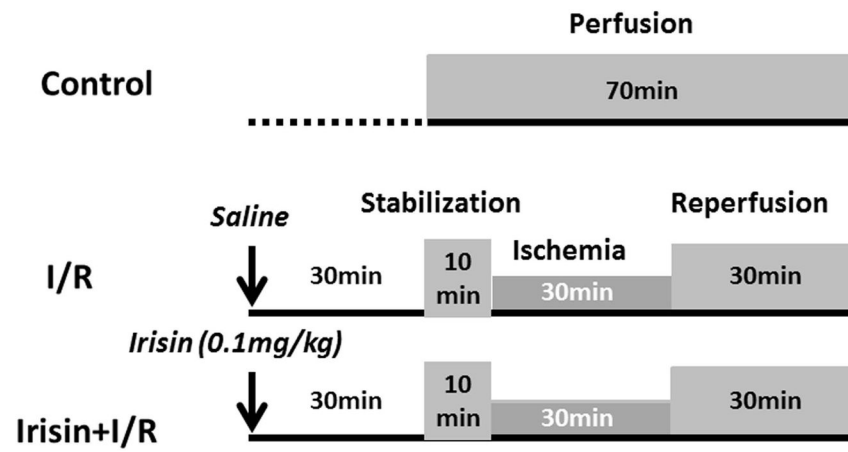
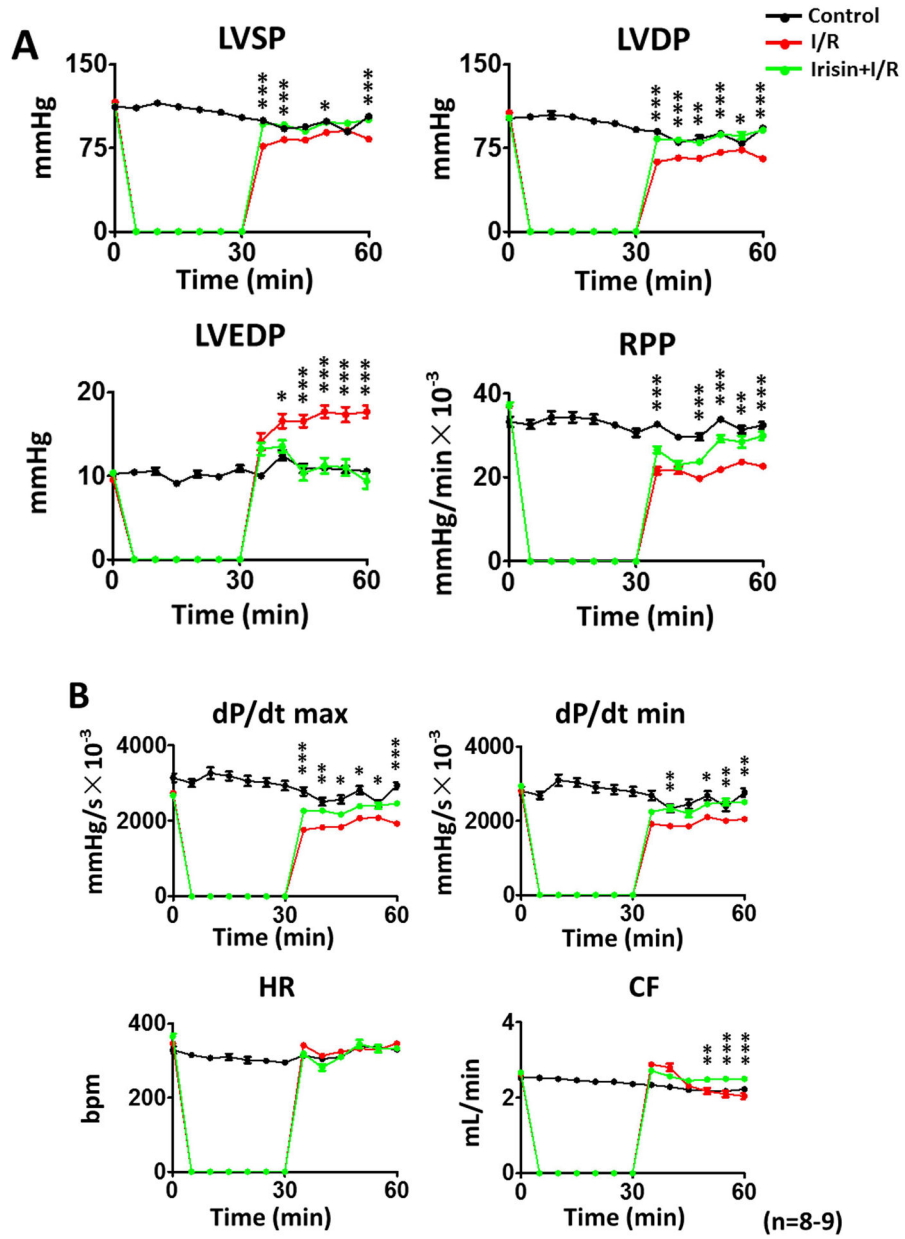


Figure 1. The diagram showing the experimental protocol of myocardial ischemia and reperfusion

I/R: ischemia/reperfusion



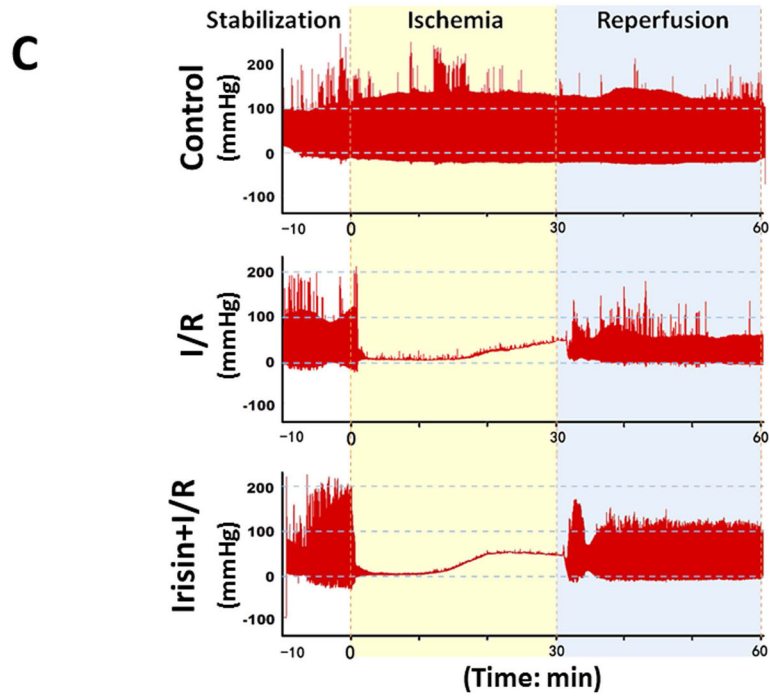


Figure 2. The effects of irisin on ventricular function in post-ischemic hearts
(A)–(B) The effects of irisin on ventricular function in LVSP, LVDP, LVDEP, LV dP/dt max, LV dP/dt min, RPP, CF, and HR during ischemia and reperfusion. Values represent as mean \pm SE (N=8–9 per group). *P<0.05, ** P<0.01, ***P<0.001 vs control I/R. **(C)** Representative left ventricular pressure records in experimental hearts subjected to I/R.

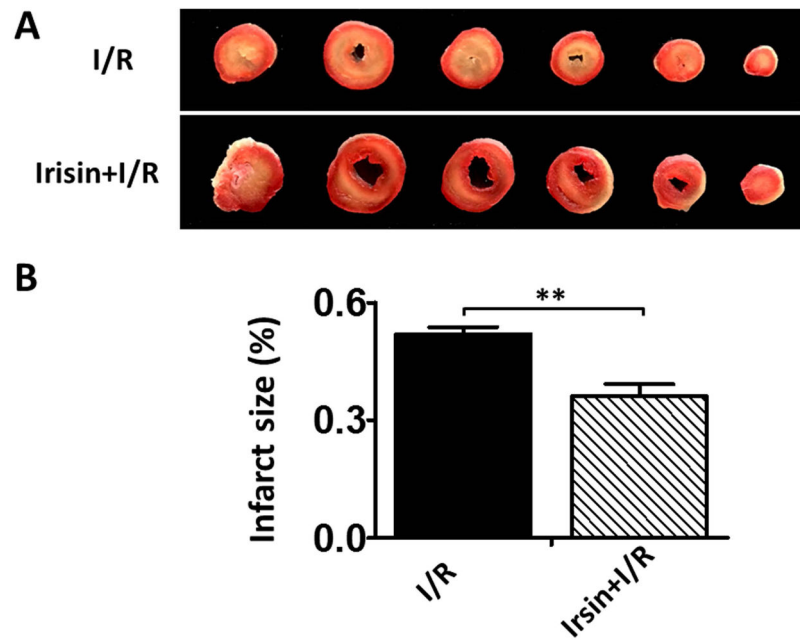
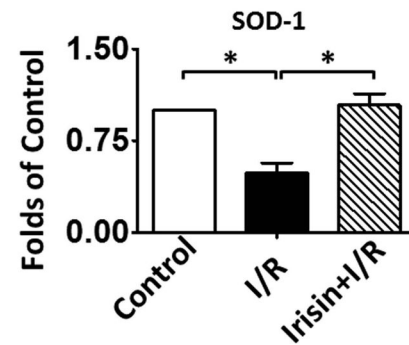
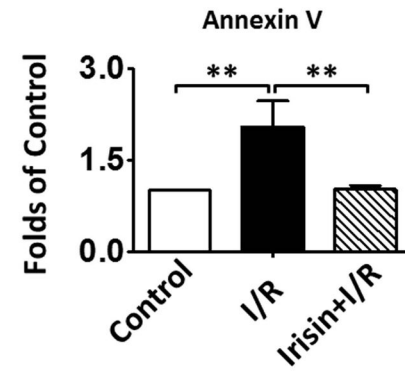
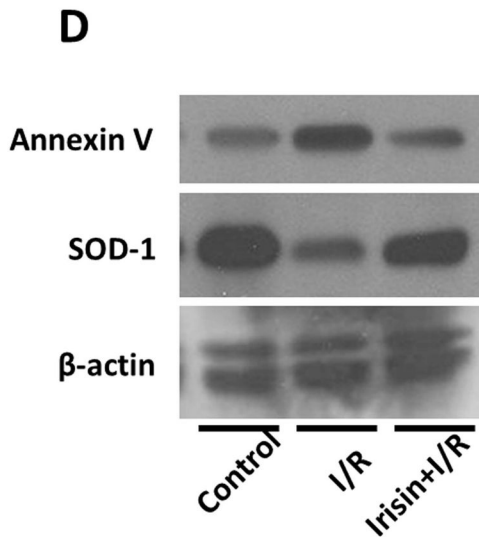
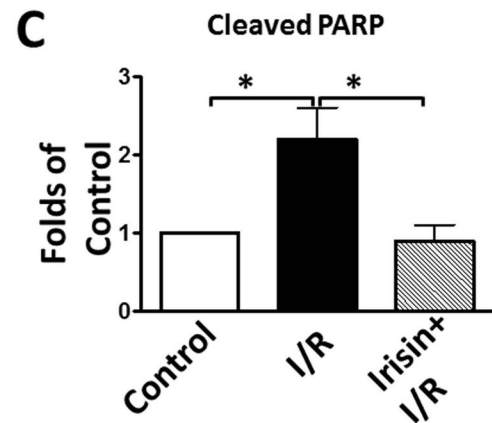
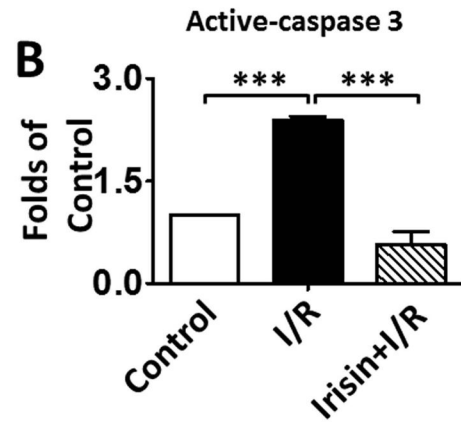
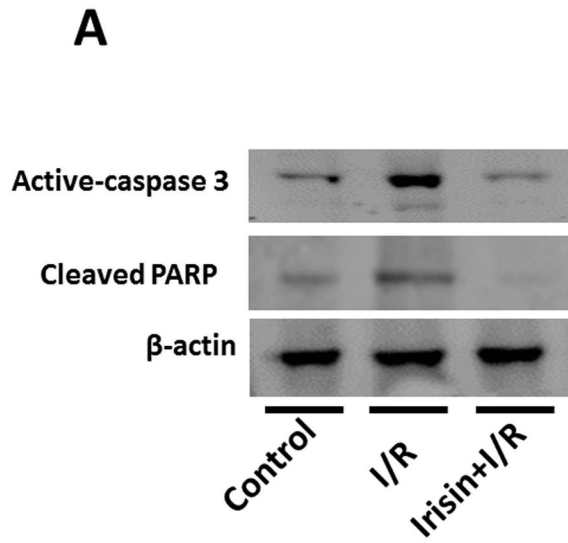
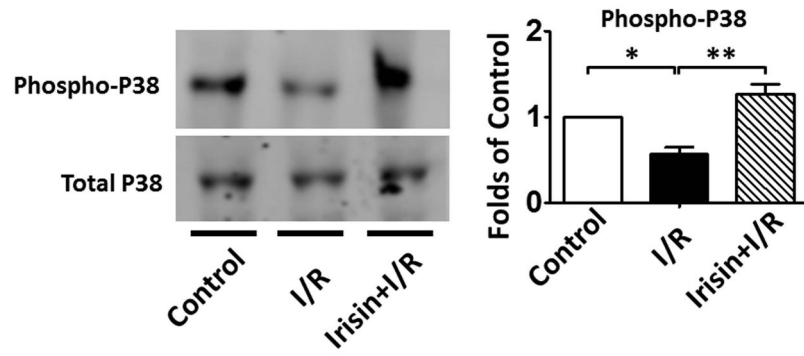
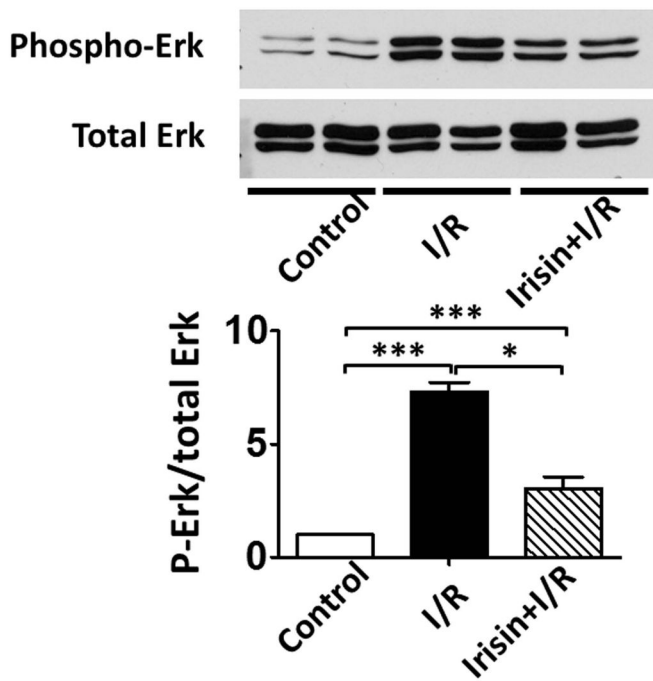


Figure 3. Irisin treatment reduced myocardial infarct size

A: Representative sections of hearts demonstrating reduction of post-ischemic infarct size 30 min after treatment with irisin. Viable areas are stained brick red, whereas infarcted areas are gray or white. **B:** Irisin treatment reduced myocardial infarct size in post-ischemic heart. There is a significant decrease in the infarcted area after irisin treatment. Values represent means \pm SE. ** $P < 0.01$ ($n = 4-5$ per group).



E**F**

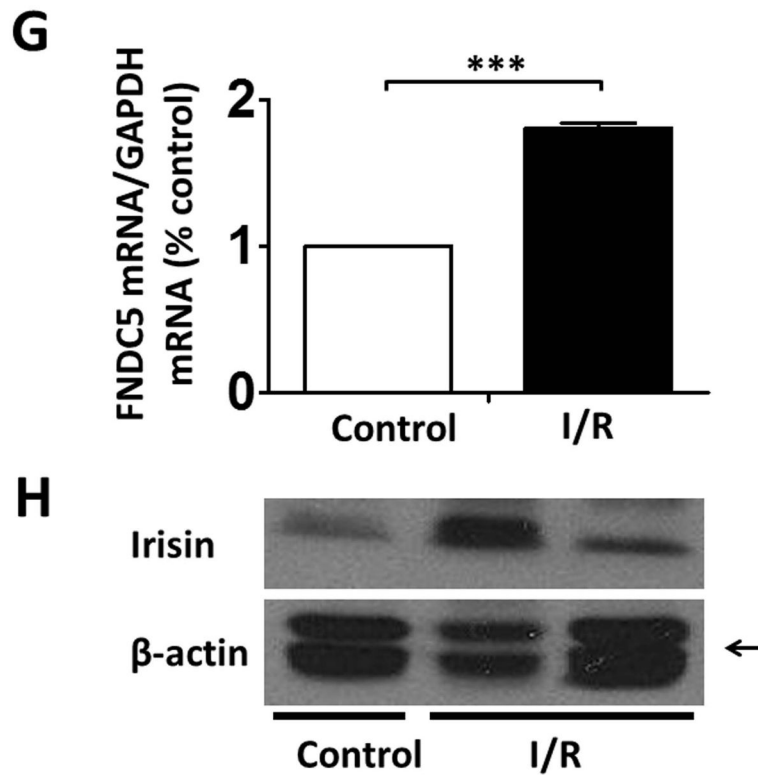


Figure 4. The effects of irisin on cellular signaling in myocardium

A; The Irisin reduced active-caspase 3 in post-ischemic heart; **B**: The bar graph shows the densitometric scanning results of active caspase-3 (n=3 per group); **C**: The bar graph shows the densitometric scanning results of cleaved PARP (n=3 per group); **D**: Irisin attenuated the contents of Annexin V in post-ischemic heart; **and**: Irisin increased the contents of SOD-1 in post-ischemic myocardium; **E**: Irisin increased p38 phosphorylation in post-ischemic myocardium; **F**: The effects of irisin on phosphorylated Erk in the post-ischemic myocardium; **G and H**: Irisin mRNA and protein levels increased in response to myocardial ischemia and reperfusion injury. The methods are described in Methods and Materials in the text.

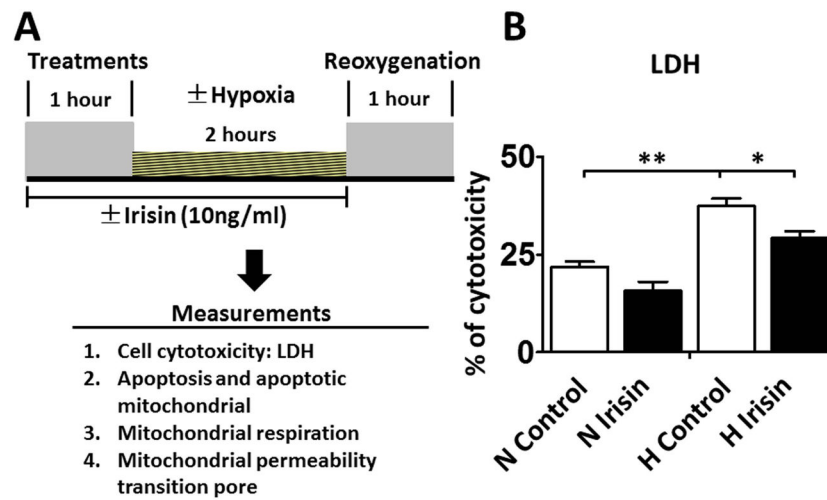


Figure 5. Irisin reduced the release of LDH in H9c2 cardiomyoblasts exposed to hypoxia/reoxygenation

A: The *in vitro* experimental protocol of hypoxia/reoxygenation in H9c2 cardiomyoblasts.

The detailed methods are described in the text. **B:** Irisin treatment attenuated LDH leakage in H9c2 cardiomyoblasts exposed to hypoxia/reoxygenation. Values represent means \pm SE (n = 3/group). *P<0.05, **P<0.01 vs control hypoxia/reoxygenation. N: Normoxia; H: Hypoxia.

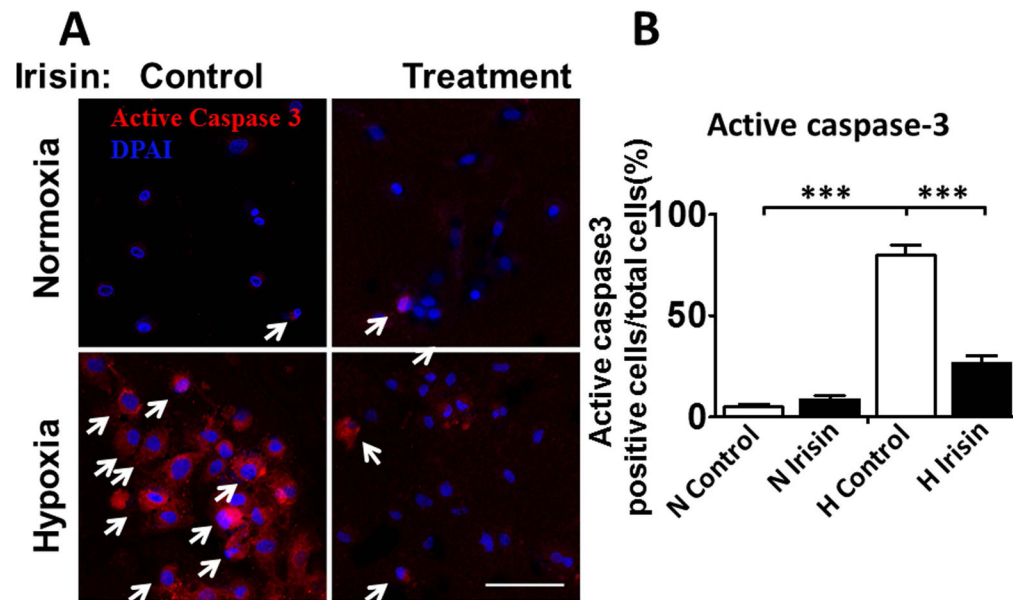


Figure 6. Irisin treatment reduced the active caspase-3-positive nuclei in cardiomyoblasts exposed to H/R

A: Representative images showing the apoptotic H9c2 cardiomyoblasts: active caspase-3-positive nuclei in red (white arrows); nuclei were stained in blue (DAPI). **B:** Quantification of active caspase-3-positive nuclei between groups. Values represent means \pm SE (n=3/group). ***P<0.001 vs control hypoxia/reoxygenation. Scale bar: 100 μ m.

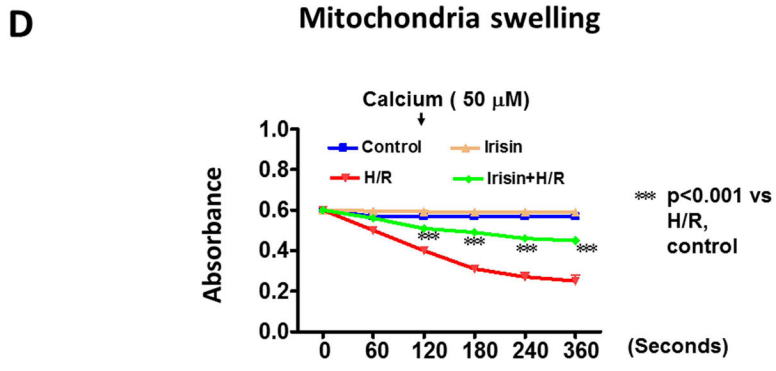
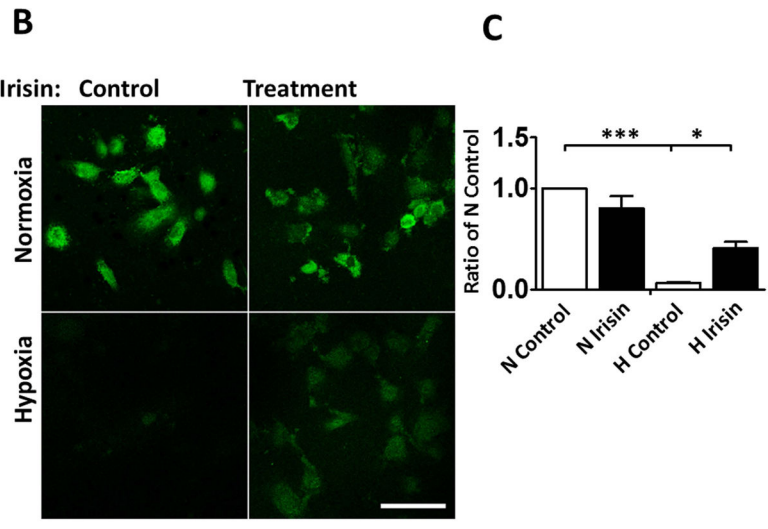
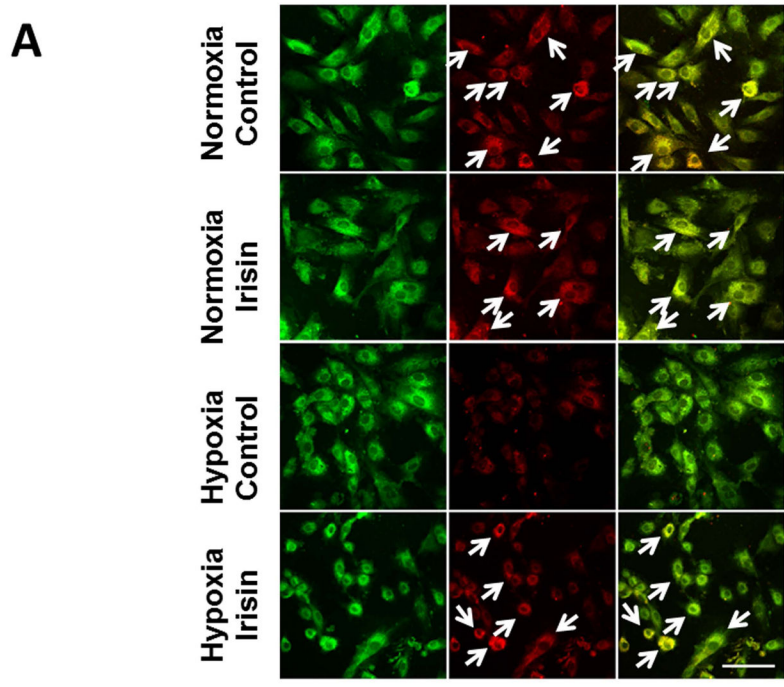


Figure 7. Effects of irisin on mitochondrial membrane depolarization and mitochondrial permeability transition pore (mPTP) opening in cardiomyoblasts exposed to hypoxia/reoxygenation

A: Irisin attenuated the mitochondrial damages in H9c2 cardiomyoblasts exposed to hypoxia/reoxygenation. Cardiomyoblast mitochondrial damage was assessed by examining mitochondrial membrane depolarization. The MitoCapture dye accumulates in the mitochondria under the condition of normoxia, emitting a red signal. In apoptotic cells, the MitoCapture diffuses into the cytoplasm and emits a green signal. **B:** Onset of mPTP is demonstrated by loss of green fluorescence signal from mitochondria. Detailed methods for measurement of mPTP was described in materials and methods. Scale bar: 100 μm . **C:** Quantitation analysis of mPTP in H9c2 cardiomyoblasts exposed to hypoxia/reoxygenation. The results represent 3–4 independent experiments counting 150–200 cells/condition. Values represent means \pm SE (n=3–4/group). *P<0.05, ***P<0.001. **D:** Quantitative analysis of mitochondrial swelling in different treatments. Values represent means \pm SE (n=3/group). N: Normoxia; H; hypoxia; R: reoxygenation; ***P<0.001.

Table 1

Baseline ventricular functional parameters.

Parameters	Control (n=9)	I/R (n=9)	Irisin+I/R (n=8)
LVSP, mmHg	111.9 ± 3.8	116.2 ± 3.1	112.4 ± 4.2
LVDP, mmHg	101.7 ± 4.6	106.7 ± 3.3	102.0 ± 4.2
LVEDP, mmHg	10.2 ± 1.0	9.6 ± 0.9	10.4 ± 0.8
RPP, mmHg/min×10 ⁻³	33.2 ± 3.7	37.0 ± 2.1	37.1 ± 2.2
dP/dt max, mmHg/s×10 ⁻³	3139.8 ± 329.2	2740.0 ± 127.5	2680 ± 153.6
dP/dt min, mmHg/s×10 ⁻³	2810.8 ± 350.1	2803.0 ± 167.1	2944 ± 162.2
HR, bpm	328.8 ± 28.5	346.7 ± 15.9	365.6 ± 22.3
CF, ml/min	2.5 ± 0.1	2.6 ± 0.1	2.7 ± 0.1

LVSP: Left ventricular systolic pressure; LVDP: Left ventricular diastolic pressure; LVEDP: Left ventricular end-diastolic pressure; RPP: Rate pressure product; CF: coronary effluent; HR: heart rate. Data are presented as means±SE (n = 8–9/per group).